Geoderma 347 (2019) 126–134

Contents lists available at ScienceDirect

Geoderma

journal homepage: www.elsevier.com/locate/geoderma

Shifts in soil microbial community functional gene structure across a 61-year desert revegetation chronosequence

Yigang Hu[a,*], Zhishan Zhang[a], Lei Huang[a], Qi Qi[b], Lichao Liu[a], Yang Zhao[a], Zengru Wang[a], Huakun Zhou[c,d], Xingyu Lv[a,e], Zhongchao Mao[a,e], Yunfeng Yang[b], Jizhong Zhou[f,g], Paul Kardol[h]

[a] Shapotou Desert Experiment and Research Station, Northwest Institute of Eco-Environment and Resources, Chinese Academy of Sciences, Lanzhou 730000, China
[b] State Key Joint Laboratory of Environment Simulation and Pollution Control, School of Environment, Tsinghua University, Beijing 100084, China
[c] Northwest Institute of Plateau Biology, Chinese Academy of Science, Xining 810008, China
[d] Qinghai Provincial Key Laboratory of Restoration Ecology of Cold Area, Xining 810008, China
[e] University of Chinese Academy of Sciences, Beijing 100049, China
[f] Institute for Environmental Genomics, University of Oklahoma, Norman, OK 73019, USA
[g] Department of Botany and Microbiology, University of Oklahoma, Norman, OK 73019, USA
[h] Department of Forest Ecology and Management, Swedish University of Agricultural Sciences, 901-83 Umeå, Sweden

ARTICLE INFO

Handling Editor: Naoise Nunan

Keywords:
Gene diversity
Microbial community
GeoChip
Revegetation
Desert

ABSTRACT

Vegetation and soil properties are crucial in shaping soil microbial communities. However, little is known about temporal changes in the functional structure of soil microbial communities to managed revegetation in desert ecosystems. Here, we adopted GeoChip 5.0-180 K, a functional gene array, to investigate the succession of soil microbial functional genes structure and potential across a 61-year revegetation chronosequence in the Tengger Desert, China. The abundance of bacterial, fungal and archaeal genes generally increased during succession. However, variation in α-diversity of microbial functional genes and signal intensity of most C-, N- and P-cycling related genes showed hump-shaped patterns along the successional gradient. Although microbial functional structure changed during succession, these revegetation sites shared a high percentage of functional genes and nestedness-resultant component dominantly determined β-diversity. Furthermore, microbial functional structure significantly correlated with crustal and shrub coverage, thickness and mass of crusts, soil fine particles, total C, total P and the ratios of C to N and C to P. The canonical correspondence analysis (CCA) and CCA-based variation partitioning analysis showed that environmental variables explained 56.6% and 85.3% of the variance in overall microbial functional genes, respectively. These results indicate that vegetation development, especially the colonization and development of soil crusts together with changes in soil abiotic properties, play key roles in driving the functional shifts in soil microbial community structure after desert revegetation.

1. Introduction

Deserts occupy about a quarter of the global land surface and are characterized by low plant cover, bare soil and aeolian sandy conditions. Biological soil crusts (BSCs), a complex of cryptogams and microorganisms cemented with soil particles, are a major component of desert ecosystems, covering as much as 70% of the surface area in the Mojave Desert (Zaady and Bouskila, 2002; Belnap and Lange, 2003). Due to the key functions in C cycling, N-fixation, eco-hydrological processes and stabilization of deserts (Eldridge and Greene, 1994; Belnap and Lange, 2003; Elbert et al., 2012), BSCs play important roles in driving vegetation succession and soil development in desert ecosystems (Li et al., 2007a, 2007b). According to previous studies in a revegetated region of the Tengger Desert, China, BSCs colonize and establish in the first several years after revegetation, thereby stabilizing the soil surface and enhancing further ecosystem succession. Many changes in plant community composition and soil properties occur in the following decades (Li et al., 2004, 2007a). After 50 years of succession, BSCs make up > 80% of the sandy surface and shift from cyanobacteria-dominated crusts to moss and lichen-dominated crusts (Li et al., 2006). These changes in the composition of BSCs result in improvement of soil nutrient levels and alteration of plant community structure, such as the establishment of herbaceous plants and a decrease in the abundance of shrubs (Li et al., 2007b).

Microorganisms play integral and unique roles in driving soil biogeochemical cycles of carbon (C), nitrogen (N), phosphorus (P), sulfur

* Corresponding author.
E-mail address: huyig@lzb.ac.cn (Y. Hu).

https://doi.org/10.1016/j.geoderma.2019.03.046
Received 1 June 2018; Received in revised form 26 March 2019; Accepted 28 March 2019
Available online 05 April 2019
0016-7061/

(S) and metals that are crucial to ecosystem functioning (Falkowski et al., 2008). In soil microbial ecology, one of the central questions is how soil microbial community respond to ecological succession (Fitter et al., 2005; Little et al., 2008). In the past few years, several studies have addressed the succession of soil microbial communities after desert revegetation (Grishkan et al., 2015; Zhang et al., 2016a; Zhang et al., 2016b; Liu et al., 2017a, 2017b). However, these studies have largely focused on changes in taxonomic features of microbial communities, while it remains unclear how the functional composition and abundance of microbial communities respond to the changes in vegetation composition and soil physicochemical properties. Furthermore, the underlying drivers that control microbial community succession are not well understood (Knelman et al., 2014).

Analysis of microbial functional genes can shed light on how microbial community functions changes in response to shift in abiotic and biotic conditions (Chan et al., 2013; Freedman et al., 2013; Reeve et al., 2010; Yang et al., 2014). Microarray-based analysis (e.g., GeoChip) can identify microbial functional genes relevant to metabolic pathways, energetics and regulatory circuits (e.g. N-cycling) associated with key soil ecosystem processes (Zhou et al., 2011; Yang et al., 2014). GeoChip can target key genes involved in the biogeochemical cycles of C, N, P and S as well as other degradation genes for the common contaminant degrading genes and antibiotic resistance genes (Van Nostrand et al., 2016). As such, the GeoChip method has been used to link microbial functional structure with environmental processes across many ecosystems (Zhou et al., 2008; Freedman et al., 2013; Yang et al., 2014). Owing to its ability to obtain quantitative measurements, GeoChip technology can provide valuable insights into changes of soil microbial functional structure and potential at the functional gene level during ecosystem succession.

In this study, we investigated changes in soil microbial community abundance and functional gene compositions and abundances using qPCR and GeoChip 5.0-180 K across a 61-year revegetation chronosequence in the Tengger desert, China. Our objectives were to 1) reveal how soil microbial community and functional gene structure respond to revegetation and soil development in the desert environment, and 2) examine the relationships of microbial functional structure with abiotic and biotic environmental variables. Previous studies have shown that the abundances of soil microbial communities and functional gene potential depend on the successional age and soil development (Kandeler et al., 2006; Brankatschk et al., 2011; Liu et al., 2017b), with soil nutrient availability as a driving limiting factor (Lozupone and Knight, 2007; Jesus et al., 2009; Yang et al., 2014). Accordingly, we hypothesized that soil microbial biomass and functional gene diversity as well as functional potential of C-, N- and P- cycling genes increased during succession.

2. Materials and methods

2.1. Study site

This study was conducted at the Shapotou Desert Experiment and Research Station (SDERS) of the Chinese Academy of Sciences (104°57′E, 37°27′N), located at the southeastern edge of the Tengger Desert. This area represents a typical ecotone between desertified steppe and sandy desert. Our study site is situated at a transitional belt between oasis and desert at an elevation of 1330 m a.s.l. The mean annual temperature is 10.0 °C with a minimum monthly mean temperature of −6.9 °C in January and a maximum of 24.3 °C in July. The mean annual rainfall between 1956 and 2009 was 188.2 mm, with about 80% of rainfall occurring between May and September. A northwest wind prevails with an average annual velocity of 2.6 m s^{-1}, and the annual potential evaporation is about 2900 mm. The soils are composed of fine sands with uniform physicochemical properties and rather low moisture content ranging from 3% to 4%. The soil type is an aeolian sandy soil. Detailed information on the dominant vegetation can be found in Li et al. (2007b).

During the period from 1956 to 1991, a non-irrigated sand-fixing vegetation protection system was established at the both sides of the Baotou-Lanzhou railway to prevent sand burial. The protection system was established in 1956, 1964, 1981, 1987 and 1991 by planting xerophytic shrubs (*Artemisia ordosia Krasch*, *Caragana korshinskii Kom*. and *Caragana micro-phylla Lam*.) within 1 m × 1 m straw-checkerboards to stabilize the dune surfaces (Li et al., 2004). Details on how straw-checkerboards were established and how the shrubs were planted can be found in Li et al. (2007b). In brief, straw-checkerboards with a height of 0.15–0.2 m above the ground were built on the dune surface, and then 2-year-old seedlings of xerophytic shrubs mentioned above were planted in a mixed way with the same species allocation and density (16 individuals per 100 m^2). Over the past decades, this system has shifted from a simple vegetation type with the three planted species to a much more complex system dominated by artificially planted shrubs, herbaceous plants and BSCs (Li et al., 2007b). In 1989 and 2012, two 1-ha areas at SDERS were revegetated as described above.

2.2. Soil sampling and measurement of physiochemical variables

In June 2017, we collected soil samples from different revegetation sites established in 1956 (61Y), 1964 (53Y), 1981 (36Y), 1989 (28Y) and 2012 (5Y) for qPCR and GeoChip microarrays and measurements of biotic and abiotic variables, while the adherent moving sand (MS) was considered as the control. The sampling sites 61Y, 53Y, 36Y and MS are located north of the railway and are characterized by highly variable topography due to the presence of sand dunes, while the 28Y and 5Y sites are located south of the railway and have been flattened before revegetation. To avoid confounding effects of topography at each sampling site, three 1 m × 1 m plots were randomly selected at the flat area between sand dunes. The nearest distance from the plots to the crown of shrubs was > 30 cm to avoid rhizosphere effects. Five soil cores (4.5 cm diameter × 5 cm depth) were taken at the corner and center of each plot and then combined to generate one composite soil sample pre plot. Thus, three soil samples were collected from each sampling site. The algae and lichens on the soil surface were removed using a knife, after which the soil samples were put on ice and taken back to laboratory. In the lab, the soil samples were then thoroughly mixed and sieved through 2 mm mesh to remove visible roots and mosses. The sieved fresh soils for GeoChip microarrays were stored at −80 °C until DNA extraction or at 4 °C to determine mineral nitrogen concentrations. Soil samples for measurements of other physiochemical variables were air-dried at room temperature.

Within each sampling site, three 10 m × 10 m plots were randomly selected to evaluate the coverage of shrubs. In each 10 m × 10 m plot, we established three 1 m × 1 m plots to evaluate the coverage and mass of BSCs. We collected BSCs by pushing a 4.5 cm diameter PVC collar into the soil after wetting the soil surface with distilled water to prevent breakage damage of BSCs. The BSCs were then taken back to the laboratory and dried at 80 °C for 24 h. All soil particles were carefully removed and BSC biomass was weighed. The thickness of BSCs was measured using a flexible rule during soil sampling. Particle size was determined by the pipette method (Nanjing Institute of Soil Sciences, 1978). Soil pH was determined in a 1:5 soil and water slurry. Soil total C (TC) was determined by the dichromate oxidation method of Walkley–Black (Nelson and Sommers, 1996). Total N (TN) was measured with the Kjeldahl method using a Kjeltec System 1026 distilling unit (Tecator AB, Höganäs, Sweden) (AOCS, 1989). Total phosphorus (TP) was determined colorimetrically after $HClO_4$–H_2SO_4 digestion (Liu et al., 1996). Soil ammonia and nitrate were extracted by shaking soil (40 g) in 100 mL 2 M KCl within two days after the soil samples were collected and then filtered using Whatman #40 filter paper. Ammonia and nitrate concentrations were determined colorimetrically on a segmented flow analyzer (AA3, Seal Analytical, Germany).

2.3. DNA extraction, purification and quantitation

We performed DNA extraction, purification and labeling as described by Van Nostrand et al. (2016) and Yang et al. (2017). Briefly, DNA extraction from soil samples was performed using the FastDNA SPIN Kit for soil (MP Biomedical, Carlsbad, CA, USA). DNA quality was assessed by determining 260/280 and 260/230 nm absorbance ratios (above 1.7) with a NanoDrop ND-1000 Spectrometer (NanoDrop Technologies, Inc., Wilmington, DE, USA). Whole community DNA amplification was performed using the Templiphi 500 kit (GE Healthcare, Piscataway, NJ, USA) and a modified reaction buffer containing spermidine (0.1 mM) and single stranded binding protein (267 ng ml^{-1}) to improve amplification efficiency. The amount of DNA was quantified via a PicoGreen method (Ahn et al., 1996) with a FLUO star Optima (BMG Labtech, Jena, Germany).

2.4. Quantitative PCR

Quantitative PCR (qPCR) was used to determine the absolute abundance of bacteria, fungi and archaea with selected primer pairs (Table S1). The qPCR reaction mixture (20 μL) contained 10 μL of ChamQ SYBR Color qPCR Master Mix (Vazyme Biotech Co., Ltd., China), 0.8 μL of each forward and reverse primers (5 μM), 1 μL of template DNA (5 ng/μL) and 7.4 μL ddH_2O. Thermocycling consisted of initial denaturation at 95 °C for 5 min followed by 40 cycles of 95 °C for 5 s, annealing temperature of 55 °C for 16 S rDNA and 58 °C for ITS and Arch for 30s and 72 °C for 40 s. All qPCRs were performed in triplicate and assayed on a StepOne Real-Time PCR System (ABI 7500, Applied Biosystems, America). The gene copy numbers of bacterial 16S rDNA, archaeal 16S rDNA and fungal ITS genes were calculated using a regression equation for converting the cycle threshold (Ct) value to the known number of copies in the standards.

2.5. GeoChip 5.0 microarray

The GeoChip 5.0-180 K microarray (SurePrint G3 custom, Agilent Technologies, Santa Clara, CA) used in this study contains 161,961 oligonucleotide probes targeting > 300 gene families, which are listed at http://www.ou.edu/ieg/tools. Labeling, hybridization and data processing was performed as described by Van Nostrand et al. (2016). Briefly, 1.0 μg DNA was labeled with the fluorescent dye Cy-3 (GE Healthcare, Chicago, IL, USA) using random primers (Fisher Scientific, Waltham, MA, USA; random hexamers, 3 μg/μL) and Klenow (Imer; San Diego, CA; 40 U/mL) and hybridized to the GeoChip microarray at 67 °C and 10% formamide (Fisher Scientific, Waltham, MA, USA) for approximately 16 h and then imaged on a Nimblegen MS200 microarray scanner at 100% photomultiplier tube and laser power (Roche-Nimblegen, Madison, WI, USA). The images were processed using the Agilent Feature Extraction program that designates values for probe signal intensities and background (noise) signal intensities based on the scanned images.

2.6. Data analyses

Raw GeoChip data were analyzed using a data analysis pipeline as previously described by Yang et al. (2014). The following four steps were performed: (i) poor-quality spots were removed when the signal-to-noise ratio (SNR) was smaller than 2, or the signal smaller than 200, or smaller than 1.3 times of the background; (ii) raw GeoChip data were normalized by signal intensity, that is, each spot was divided by the total intensity of its microarray and then multiplied by the average value of the microarray's total intensity; (iii) a minimum of two valid values for each gene was required in a triplicate set of each sampling site; and (iv) GeoChip data were ln-transformed.

One-way analysis of variance (ANOVA) and Least Significance Difference (LSD) (SPSS 16.0 Inc., Chicago, IL, USA) were adopted to examine the difference in environmental variables, and the richness, α-diversity indices (Shannon index and Simpson index) and normalized signal intensity of functional genes among sampling sites. Nonparametric tests were used to examine the differences among sites for data that failed to meet the assumptions of normality of residuals and homoscedasticity. We analyzed the GeoChip data using a GeoChip data analysis pipeline (http://ieg.ou.edu/microarray/) as previously described (Yang et al., 2014; Van Nostrand et al., 2016). In brief, detrended component analysis (DCA) was used to determine the changes in the overall functional gene composition within the microbial communities using the decorana function in R. A PERMANOVA test using the *adonis* function was adopted to examine the differences in microbial community function among sampling sites. Mantel tests, canonical correspondence analysis (CCA) and variation partitioning analysis (VPA) were used to evaluate the linkages between soil microbial functional gene composition and environmental variables. Mantel tests were performed using Euclidean distance metrics, and CCA and VPA were performed using the cca function in R. All these analyses were performed using the Vegan package in R v. 3.3.3. To correct Type I error inflation, Bonferroni corrections were applied to adjust all *P*-values using p.adjust function in the Hmisc package in R. For CCA, environmental variables correlated with other factors were removed when the variable had a variation inflation factor value larger than 20. VPA was applied to split the environmental variables selected by CCA into three groups (vegetation properties, soil physical properties and soil chemical properties). Multiple-site Sorensen dissimilarity (β_{SOR}) and its components of turnover (β_{SIM}, i.e. gene replacements between sites) and nestedness-resultant dissimilarities (β_{SEN}, i.e. gene gains/losses from site to site) of overall genes and C-, N- and P-cycling related genes were calculated using the betapart package in R as described by Baselga and Orme (2012). The ratio of β_{SNE} to β_{SOR} indicates that gene turnover predominantly determines β diversity when $\beta_{SNE}/\beta_{SOR} < 0.5$, and nestedness-resultant is the dominant component when $\beta_{SNE}/\beta_{SOR} > 0.5$ (Dobrovolski et al., 2012).

3. Results

3.1. Variations in vegetation and soil properties

Nearly all sites showed an increase in the coverage, thickness and biomass of BSCs with time since revegetation, despite occasional non-significant differences between sites. Similarly, increases in silt content, clay content, EC, TC, TN, TP, nitrate and C/N, C/P and N/P ratios were observed over time, while the sand content decreased. Shrub coverage significantly increased in the first 28 years and decreased thereafter (Table S2).

3.2. Distribution patterns of microbial community and overall functional genes

Across all sites, gene copy numbers of bacteria, based on qPCR data, was on average 137.6 (ranging from 23.7 to 326.7) times higher than that of fungi, while the numbers of archaea were on average 3.3 (ranging from 1.3 to 5.5) times higher than that of fungi. Although there were no significant differences in fungal gene copy numbers among sites 28Y, 53Y and 61Y, the abundances of bacteria, fungi and archaea all generally increased over succession (Table 1).

A total of 94,546 genes were detected across all sites by GeoChip 5.0180 K microarrays. The richness of all microbial functional genes in the control site was the lowest with a detected gene number of 21,311, and significantly increased in the next 36 years and roughly tripled at 36Y (82,098). After that, the richness gradually decreased again. The functional α-diversity indices showed a similar temporal variation pattern. There were no significant differences in richness, and Shannon and Simpson indices of overall microbial functional genes among sites 28Y, 36Y and 53Y (Table 2).

Table 1
Gene abundance (copies/g soil) of bacteria, fungi and archaea for different revegetation sites as determined by qPCR. Data shown are mean ± se and within columns, different letters represent significant differences among sites. MS, 5Y, 28Y, 36Y, 53Y and 61Y indicate mobile sand (control), 5-, 28-, 36-, 53- and 61-year-old revegetation sites, respectively.

Site	Bacteria	Fungi	Archaea
MS	$4.5\ (0.02) \times 10^5$ e	$1.9\ (0.01) \times 10^4$ c	$2.8\ (0.1) \times 10^4$ e
5Y	$7.9\ (0.4) \times 10^8$ d	$8.6\ (1.0) \times 10^6$ b	$1.3\ (0.3) \times 10^7$ d
28Y	$11.3\ (0.5) \times 10^8$ c	$7.7\ (0.1) \times 10^6$ b	$3.4\ (0.02) \times 10^7$ d
36Y	$25.0\ (0.6) \times 10^8$ b	$18.3\ (0.5) \times 10^6$ a	$5.7\ (0.2) \times 10^7$ c
53Y	$31.6\ (0.4) \times 10^8$ b	$16.3\ (0.3) \times 10^6$ a	$6.5\ (0.1) \times 10^7$ b
61Y	$52.6\ (1.2) \times 10^8$ a	$16.1\ (0.3) \times 10^6$ a	$8.9\ (0.2) \times 10^7$ a

Table 2
Diversity indices of overall microbial functional genes for different revegetation sites. Data are mean ± standard error in the parentheses and within columns, different letters represent significant differences among sites. MS, 5Y, 28Y, 36Y, 53Y and 61Y indicate mobile sand (control), 5-, 28-, 36-, 53- and 61-year-old revegetation sites, respectively.

Site	Richness[§]	Shannon-index[#]	Simpson-index[&]
MS	21,311.3 (430.9) c	10.0 (0.04) c	21,108.6 (741.3) c
5Y	51,831.0 (1533.2) b	10.8 (0.03) b	50,373.5 (1401.3) b
28Y	74,814.7 (1295.5) a	11.2 (0.02) a	71,986.4 (1178.6) a
36Y	82,098.7 (5307.0) a	11.3 (0.07) a	78,936.9 (4962.2) a
53Y	75,411.3 (1438.3) a	11.2 (0.02) a	72,346.3 (1332.2) a
61Y	52,500.0 (1023.3) b	10.9 (0.02) b	51,096.5(923.6) b

[§] Detected average gene number.
[#] Shannon–Weiner index. Higher numbers represent higher diversity.
[&] Simpson's index. Higher numbers represent higher diversity.

Table 3
Multiple-site Sorensen dissimilarity (β_{SOR}) and its components of turnover (β_{SIM}) and nestedness-resultant (β_{SEN}) of all genes, C-, N- and P-cycling related genes.

Index	All genes	C cycling	N cycling	P cycling
β_{SOR}	0.69	0.69	0.70	0.68
β_{SIM}	0.24	0.26	0.23	0.22
β_{SNE}	0.45	0.44	0.47	0.46
β_{SNE}/β_{SOR}	0.65	0.63	0.67	0.68

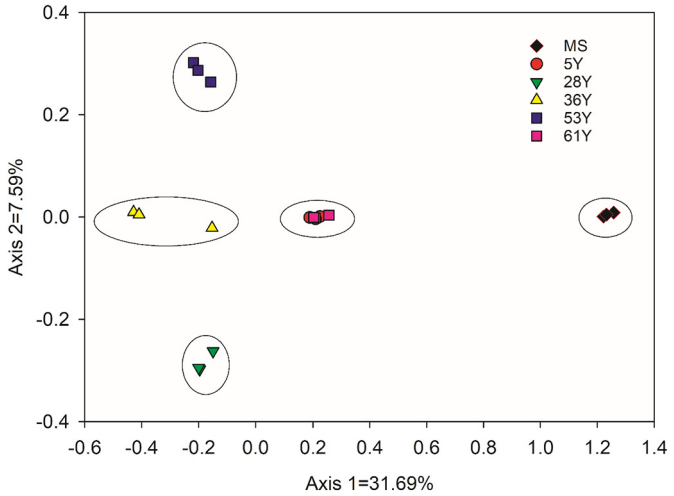

Fig. 1. Detrended correspondence analysis (DCA) of overall microbial functional structure. Percentages along the axes correspond to the amount of explained variability community composition. MS, 5Y, 28Y, 36Y, 53Y and 61Y indicate mobile sand (control), 5-, 28-, 36-, 53- and 61-year-old revegetation sites, respectively.

The dissimilarity tests revealed that microbial community functional structure in these six sites significantly differed from each other (Table S3). A high percentage (52.7–80.8%) of shared genes was observed among sites 5Y, 28Y, 36Y, 53Y and 61Y, whereas only about 25% of the genes were shared between the control site and other sites. The ratio of β_{SNE} to β_{SOR} for overall genes was higher than 0.5 (Table 3), indicating that the nestedness-resultant component predominantly determined β-diversity of overall functional genes. The highest number of unique genes was detected for site 36Y (8069), while only 63 genes were unique to site 61Y (Table S4). The DCA results of overall microbial functional structure indicated that microbial communities in sites 5Y, 28Y, 36Y, 53Y and 61Y were well separated from each other and from the control site, but microbial community functional structure at site 5Y was similar to community structure that at site 61Y (Fig. 1).

3.3. C-, N- and P-cycling related genes

The normalized signal intensity of most C-, N- and P-cycling genes was lowest in the control site and often significantly lower than in the other sites, although several genes showed no significant difference between the control site and site 5Y (e.g., *amyx* and *nplT* genes involved in starch degradation, *mct* genes involved in C-fixation, *Ftr* and *mtaB* genes involved in methanogenesis, *hzo* genes involved in anammox, and *51f1_htxA* genes involved in P oxidation). Surprisingly, the variation pattern in signal intensity of most C-, N- and P-cycling related genes showed a hump-shaped pattern with an increase during the first 36 years followed by a decrease in the following 25 years (Figs. 2, 3, 4). In most cases, there was no significant difference in the normalized signal intensity of most C-, N- and P-cycling related genes between sites 5Y and 61Y and among sites 28Y, 36Y and 53Y. However, the *51f1_htxA genes* involved in P oxidation rarely varied over succession and no significant differences were found among sites (Fig. 4). The β_{SNE} values were almost two times higher than β_{SNE}, and the ratios of β_{SNE} to β_{SOR} were higher than 0.5 for C-, N- and P-cycling related genes (Table 3), indicating that nestedness was the dominant component of their β-diversity.

3.4. Linkages between microbial functional genes and environmental variables

Mantel tests indicated that coverage, thickness and biomass of BSCs, shrub coverage, soil TC, TP, C/N, C/P, and silt and clay content were all significantly associated with microbial community functional structure with *r*-values ranging from 0.22 (TC) to 0.95 (BSCs coverage). However, microbial community functional structure was not significantly correlated with soil pH, salinity and N availability (Table 4). A significant CCA model ($P = 0.001$) was built to detect the linkages of microbial community function and main environmental variables. The first two CCA axes together explained a total of 56.6% of the variance in microbial community functional genes (Fig. 5). The results from VPA showed that these selected variables explained a total of 85.4% of the variance in microbial community functional structure, with 20.3%, 10.0% and 17.0% of the variance explained by vegetation properties, soil physical properties, and chemical properties, respectively. Significant interactions were found between vegetation properties and soil physical properties ($P = 0.007$) and between vegetation properties and soil chemical properties ($P = 0.001$), which explained 9.5% and 25.0% of the variance in microbial community functional structure, respectively (Fig. 5).

4. Discussion

4.1. Succession of soil microbial community and functional genes

The abundance estimates showed that bacteria dominated the soil

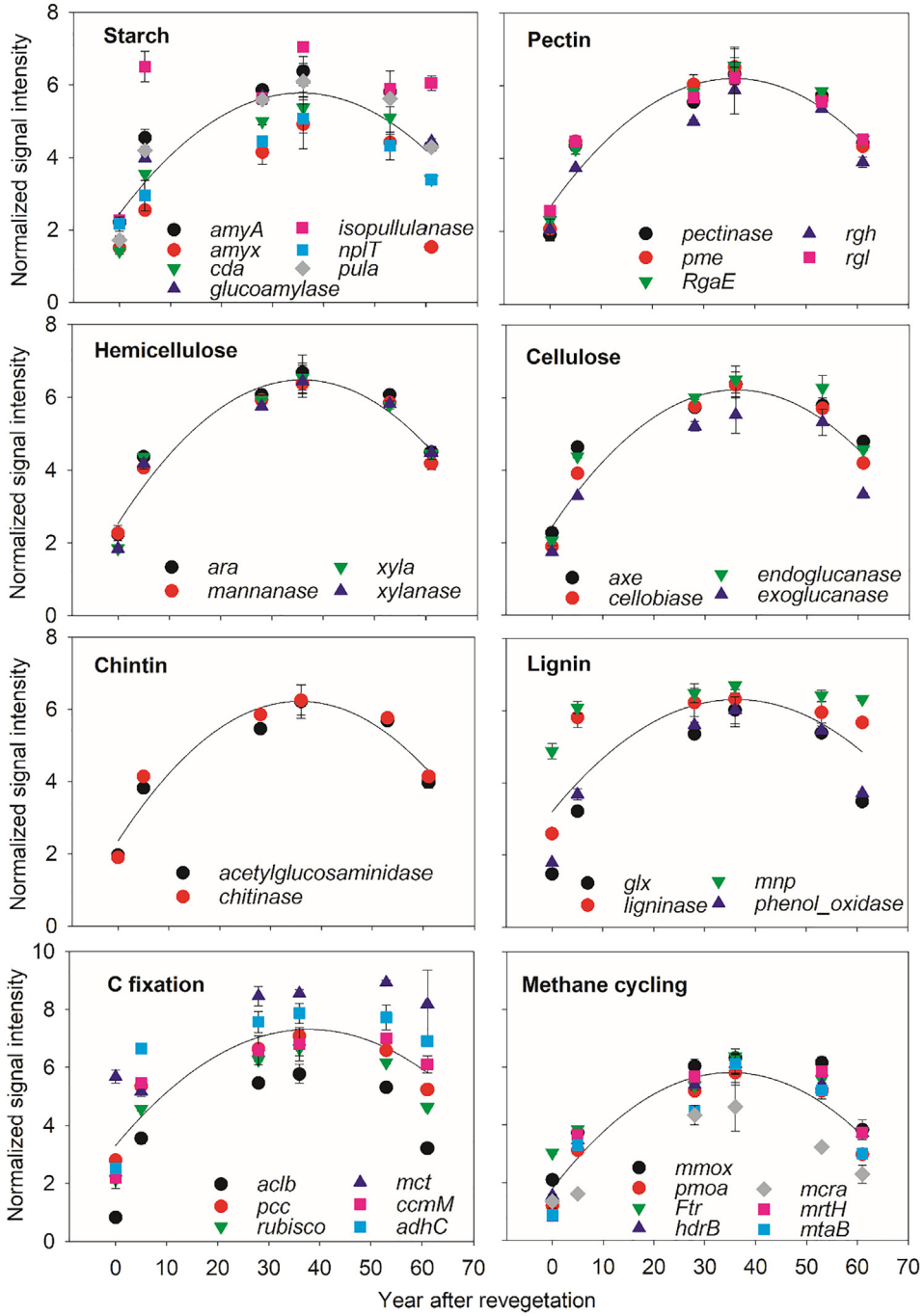

Fig. 2. Normalized signal intensity of C degradation, C fixation and methane cycling related genes over 61 years of succession. Data presented are mean ± se calculated from biological triplicates.

microbial community throughout the successional gradient, while fungi and archaea comprised a smaller proportion (Table 1), which is in line with previous observation (Liu et al., 2017a). Soil microbial communities develop in structure and function before and after plant colonization (Nemergut et al., 2007; Schmidt et al., 2008; Knelman et al., 2014), even in the earliest stages of succession with poor soil development, as has been shown for a glacier forefield (Kandeler et al., 2006; Brankatschk et al., 2011). We found that the richness of microbial functional genes doubled (Table 2) and the functional structure significantly change from the control site to the youngest 5-year old site (Fig. 1, Table S3). These findings demonstrate that soil microbial communities could rapidly develop in the early stages of desert revegetation (Liu et al., 2013). Our findings that the abundances of bacteria, fungi and archaea increased over succession (Table 1) support the previous hypothesis that soil microbial biomass increased during succession. Several reasons are attributable to the finding. First, straw checkerboards, revegetated shrubs and crustal colonization stabilized the mobile sand surface, which might create a favorable environment for microbial growth and reproduction by reducing wind and heat stresses (Liu et al., 2013). Second, vegetation development, including planted shrubs, establishment of herbs, and further crustal development enhanced soil nutrients levels (Table S2) that may help support more abundant microbial communities (Fierer et al., 2003; Tscherko et al., 2003; Kandeler et al., 2006). Third, soil microbes could also acquire nutrients and energy to meet their metabolic needs from the decomposition of straw used to stabilize the mobile sand.

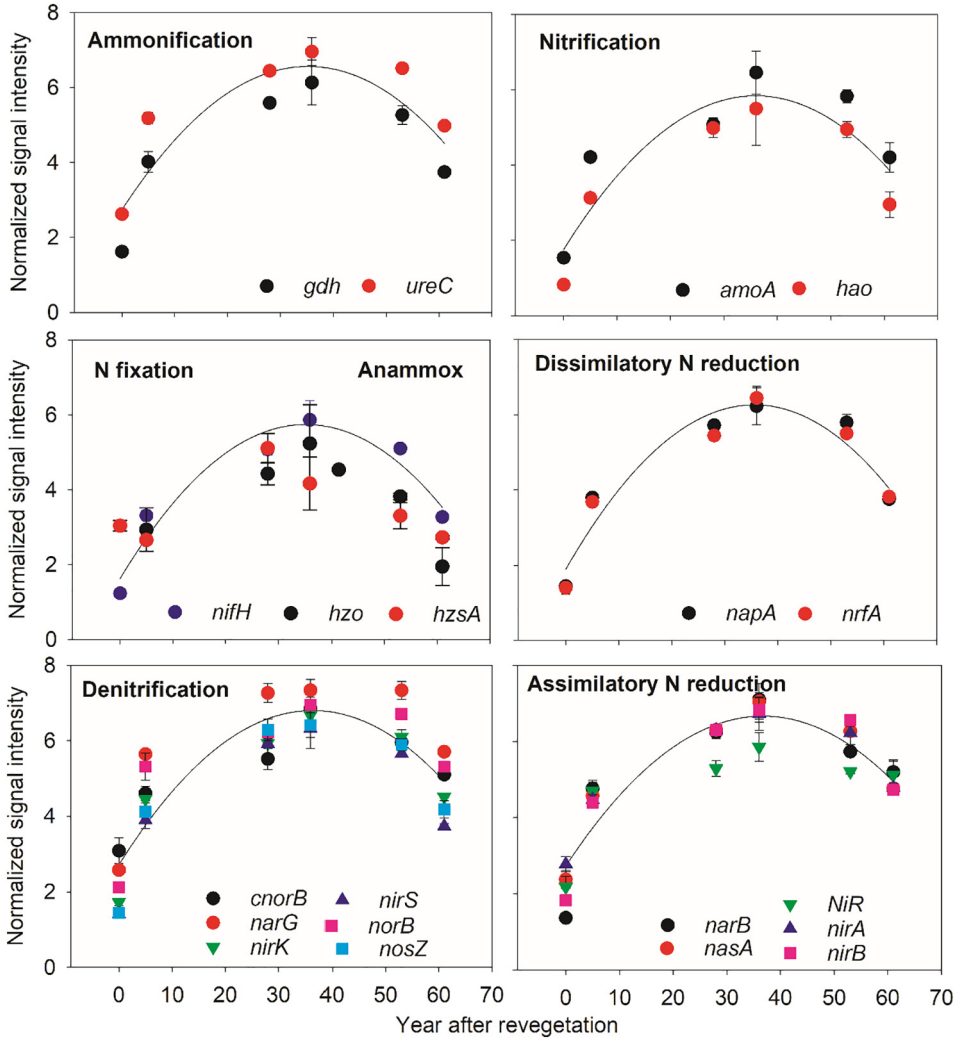

Fig. 3. Normalized signal intensity of N cycling related genes over 61 years of succession. Data presented are mean ± se calculated from biological triplicates.

Tscherko et al. (2003) showed that the diversity of microbial functional genes increased and then reached a temporary steady state during succession after a glacial retreat. However, we found that the diversity of overall microbial functional genes showed a hump-shape pattern during the 61 years of succession (Fig. S1), which was not the case for the variations in bacterial and archaeal abundances. This discrepancy suggests that successional patterns of microbial functional genes differ from the pattern of microbial taxonomic abundance at the kingdom level. Moreover, the signal density of most C-, N-, P-cycling related genes also showed an increase in the first 36-year period followed by a decrease (Figs. 2, 3, 4). The decrease could be ascribed to reduced abundances of several dominant bacterial taxa including *Bacillus*, *Enterococcus*, and *Lactococcus* (Liu et al., 2017a, 2017b). Our finding that nestedness-resultant was the dominant component of β-diversity (Table 3) furtherly indicated that the decrease might be caused by loss of certain genes. Nutrient availability is an important driver of microbial succession that is sensitive to N and P (Knelman et al., 2014; Yang et al., 2014). A large fraction of nitrogen input in crusted desert soil is generally associated with N_2-fixing cyanobacteria (Belnap and Lange, 2003; Yeager et al., 2007; Wang et al., 2016). In the later successional stages, the cyanobacteria-dominated crusts have been shown to shift towards crusts dominated by lichens and mosses (Li et al., 2007b), which was supported by our observation of decreased signal density of cyanobateria related functional genes (data not shown), which in turn might weaken N fixation as suggested by the decrease in *nifH* signal density (Fig. 3). Moreover, later successional stages are typically characterized by increased P limitation (Richardson et al., 2004; Huang et al., 2012), which may further limit N-fixation (Vitousek, 1999; Vitousek et al., 2010). Although we found that soil microbial community functional structure was positively correlated with P rather than N (Table 3), N and P limitation for microbes might be accentuated due to consumption of N and P by increased BSCs biomass. These results suggest nutrient co-limitation for in microbial community succession (Knelman et al., 2014).

4.2. Drivers of microbial community functional structure

Microbial community genes structure and abundance often vary in relation to both vegetation and soil properties (Kandeler et al., 2006; Yang et al., 2014; Yue et al., 2015). Previous studies have found that vegetation productivity, soil nutrient levels, salinity and pH are important in regulating microbial functional genes structure across various ecosystems (Kandeler et al., 2006; Zhou et al., 2011; Yang et al., 2014). Our Mantel tests (Table 4) showed that BSCs development, shrub coverage, soil fine particles and nutrients level were the main controlling factors of microbial succession at the functional gene level. The insignificant role of pH in shaping microbial community functional structure might be ascribed to the small variation in soil pH among sites (Table S2). The lack of correlation between microbial functional structure and EC could be explained by high level of soil salinity, which might be beyond the shift threshold of microbial communities in response to changes in salinity. These results highlight that vegetation

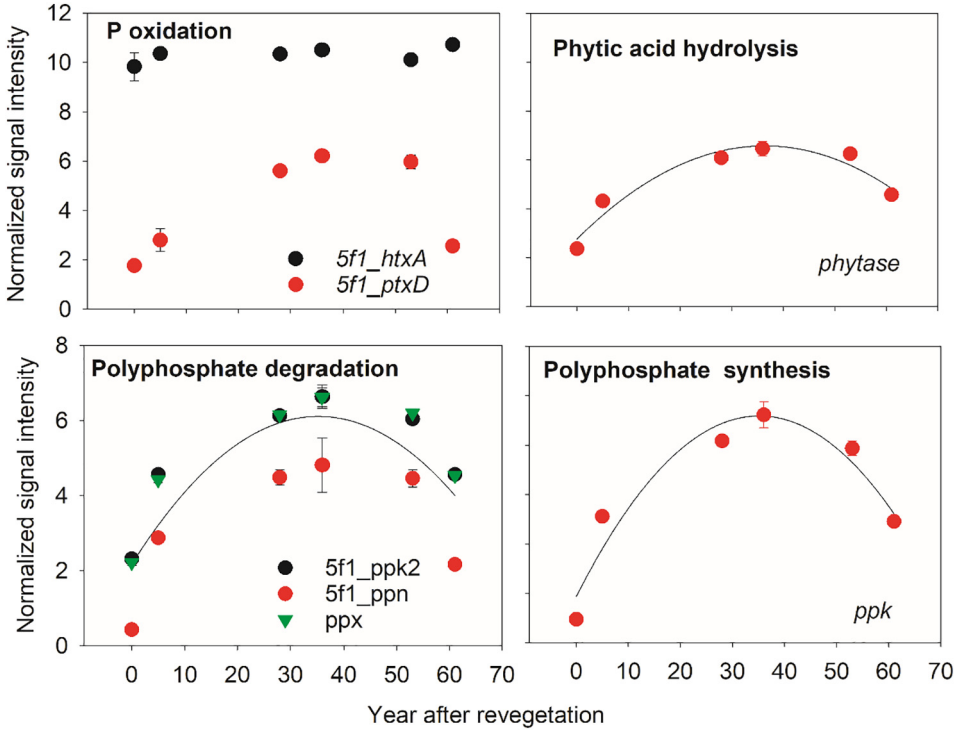

Fig. 4. Normalized signal intensity of P-cycling related genes over 61 years of succession. Data presented are mean ± se calculated from biological triplicates.

Table 4
Relationships between microbial community functional structure and environmental variables as tested by Mantel tests. BSC, biological soil crusts; EC, electrical conductivity; TC, total carbon; TN, total nitrogen; TP, total phosphorus. Significant relationships are shown in bold. ** $P < 0.01$ and * $P < 0.05$.

Environmental variables (unit)	*r*-Value	Environmental variables (unit)	*r*-Value
Crustal coverage (%)	**0.946****	TC (g kg^{-1})	**0.218***
BSCs thickness (cm)	**0.800****	TN (g kg^{-1})	0.144
BSCs mass (g cm^{-2})	**0.644****	TP (g kg^{-1})	**0.469****
Shrub coverage (%)	**0.894****	C/N	**0.856****
Silt content (%)	**0.351****	C/P	**0.463****
Clay content (%)	**0.420****	N/P	0.084
pH	0.017	Ammonia (mg kg^{-1})	−0.012
EC (us/cm)	0.184	Nitrate (mg kg^{-1})	0.075

succession coupled with soil development drove the shifts in microbial community functional structure after revegetation.

The crusted soil shares more similarities than the differences in microbial phylogenetic composition (Abed et al., 2010; Liu et al., 2017a, 2017b). Similarly, the proportion of shared functional genes among the revegetation sites was much higher than that of unique genes (Table S3), which could be attributed to high similarity of microbial phylogenetic composition in these sites (Liu et al., 2017a, 2017b). Moreover, our analysis of β-diversity (Table 3) and microbial functional structure (Fig. 1, Table S2) indicate that gene gains/losses is the main driver of microbial community functional succession in desert soil. The two axes of CCA totally explained 56.6% of the variance in community genes, which is comparable with previous finding by Yang et al. (2014) and much higher than other GeoChip studies (Liang et al., 2011; Yue et al., 2015). Notably, vegetation properties and soil chemical properties explained nearly twice as much of the variance in microbial functional genes structure than soil physical properties (Fig. 5), indicating that vegetation properties are more important than soil physical properties in driving microbial succession. Changes in vegetation composition may be associated with a shift in C inputs into soil by means of shoot and root litter and root exudates. The increased mortality of shrubs over succession (Li et al., 2007b) would reduce the input of low-recalcitrant C input from litters into the soil, which might result in the reduction of the signal intensities of microbial genes involved in the degradation of lignin, chitin and cellulose in the latter successional stages. However, we note that it is difficult to clearly isolate individual effects of vegetation and soil properties on soil microbial succession due to their close linkages and possible interactions.

4.3. Implications of microbial community functional potential

Space-for-time substitutions have been widely used to infer long-term temporal trends in microbial succession across ecosystems (Tscherko et al., 2003; Kandeler et al., 2006; Brankatschk et al., 2011; Zhang et al., 2016a; Liu et al., 2017a, 2017b). Here, we report the profiling of microbial community abundances and functional gene structure and potential, which provides valuable insights for their successional patterns in the desert. The initial soil property and revegetation protocols in our study meet the preconditions of the space-for-time substitutions approach, generating reliable results. Our findings partially supported the hypothesis that soil bacterial, fungal and archaeal abundance, functional genes diversity and functional potential of most C-, N- and P-cycling related genes increase during succession. However, a decrease in both diversity of overall functional genes diversity and functional potential of most C-, N- and P-cycling related genes in the following 25 years is surprising, and implies that C-, N- and P-cycling processes might slow down in the latter successional stages. However, it is important to note that our DNA-based analyses inform on functional potentials rather than actual microbial activities. Microbial composition, abundance and functional potential are important in driving a variety of ecosystem processes (Yang et al., 2014; Zhou et al., 2011). For future studies, it is therefore necessary to combine both microbial taxonomic community and functional potential with biogeochemical cycling processes (such as ecosystem respiration and N fixation) to address how microbial structure and functions control such ecological processes during succession.

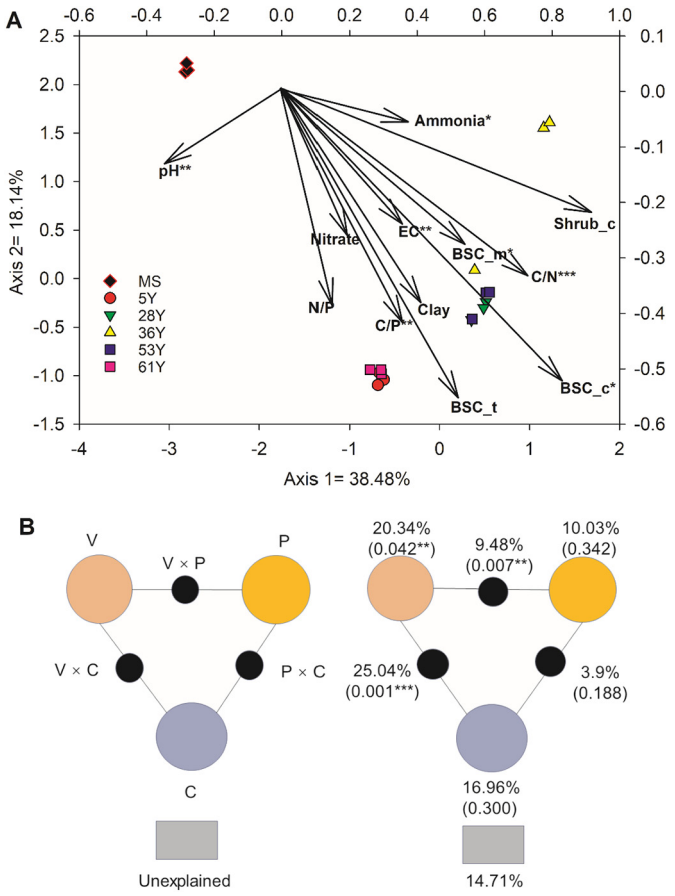

Fig. 5. Canonical correspondence analysis (CCA) of microbial functional structure and environmental variables (A). Shrub_c, BSC_m, BSC_c and BSC_t represent shrub coverage, BSCs mass, BSCs coverage and BSCs thickness, respectively. Percentages along the axes correspond to the amount of explained variability community composition, and the relationship is significant ($P < 0.05$). *, ** and *** indicate significance at $P < 0.1$, $P < 0.05$ and $P < 0.01$, respectively. MS, 5Y, 28Y, 36Y, 53Y and 61Y indicate mobile sand (control), 5-, 28-, 36-, 53- and 61-year-old revegetation sites, respectively. Variation partitioning analysis of microbial community function diversity among three groups of variables (B): 1) vegetation properties (V) cover the thickness, coverage and biomass of BSCs, 2) soil physical properties (P) cover clay content, pH and EC, and 3) soil chemical properties (C) cover ammonia, nitrate and the ratio of N to P, and their interactions (V × P, V × C, P × C and V × P × C). The values in parentheses are *P*-values.

5. Conclusions

This study described soil microbial succession in functional gene structure and potentials related to C-, N- and P-cycling across a 61-year chronosequence in a temperate revegetated desert at the functional gene level. The most important finding is that microbial community functional gene structure and potentials rapidly changed after revegetation, even in the earliest stages of succession. This indicates that microbial functional structure might be used as a potential indicator to evaluate the stability of managed revegetation desert ecosystem. Different vegetation sites shared a high percentage of genes and microbial succession appeared to operate through gains/losses of certain genes rather than genes replacement. This sheds new light on the successional pattern of soil microbial communities in the temperate desert. Our findings that soil microbial functional community structure was strongly related to several plant ecological variables and soil physiochemical variables highlight that changes in vegetation and soil properties were the key factors in driving microbial succession in the desert ecosystems. Further studies are needed to better link soil microbial taxonomic composition and functional potential with biogeochemical cycling processes to address how microbial composition and structure control C-, N- and P cycling processes over succession.

Acknowledgements

We thank Joy D. Van Nostrand for help with data analysis and manuscript editing. This work was financially supported by the National Key Research and Development Program of China (2017YFC0504301), the Natural Science Foundation Committee of China (41101081, 41471434 and 41771105) and Qinghai Innovation Platform Construction Project (2017-ZJ-Y20).

Appendix A. Supplementary data

Supplementary data to this article can be found online at https://doi.org/10.1016/j.geoderma.2019.03.046.

References

Abed, R.M., Kharusi, K.S., Schramm, A., Robinson, M.D., 2010. Bacterial diversity, pigments and nitrogen fixation of biological desert crusts from the Sultanate of Oman. FEMS Microbiol. Ecol. 72 (3), 418–428.
Ahn, S.J., Costa, J., Emanuel, J.R., 1996. PicoGreen quantitation of DNA: effective evaluation of samples pre- or post-PCR. Nucleic Acids Res. 24, 2623–2625.
AOCS, 1989. Official Methods and Recommended Practices of the American Oil Chemists' Society, 4th ed. AOCS, Champaign, IL.
Baselga, A., Orme, C.D.L., 2012. Betapart: an R package for the study of beta diversity. Methods Ecol. Evol. 3, 808–812.
Belnap, J., Lange, O.L., 2003. Biological Soil Crusts: Structure, Function, and Management. Springer-Verlag, Berlin, pp. 3–30.
Brankatschk, R., Töwe, S., Kleineidam, K., Schloter, M., Zeyer, J., 2011. Abundances and potential activities of nitrogen cycling microbial communities along a chronosequence of a glacier forefield. ISME J. 5, 1025.
Chan, Y., Van Nostrand, J.D., Zhou, J., Pointing, S.B., Farrell, R.L., 2013. Functional ecology of an antarctic dry valley. Proc. Natl. Acad. Sci. 110, 8990–8995.
Dobrovolski, R., Melo, A.S., Cassemirom, F.A.S., Diniz-Filho, J.A.F., 2012. Climatic history and dispersal ability explain the relative importance of turnover and nestedness components of beta diversity. Glob. Ecol. Biogeogr. 21, 191–197.
Elbert, W., Weber, B., Burrows, S., Steinkamp, J., Büdel, B., Andreae, M.O., Pöschl, U., 2012. Contribution of cryptogamic covers to the global cycles of carbon and nitrogen. Nat. Geosci. 5, 459–462.
Eldridge, D.J., Greene, R., 1994. Microbiotic soil crusts - a review of their roles in soil and ecological processes in the rangelands of Australia. Soil Res. 32, 389–415.
Falkowski, P.G., Fenchel, T., Delong, E.F., 2008. The microbial engines that drive Earth's biogeochemical cycles. Science 320 (5879), 1034–1039.
Fierer, N., Schimel, J.P., Holden, P.A., 2003. Variations in microbial community composition through two soil depth profiles. Soil Biol. Biochem. 35, 167–176.
Fitter, A.H., Gilligan, C.A., Hollingworth, K., Kleczkowski, A., Twyman, R.M., Pitchford, J.W., 2005. Biodiversity and ecosystem function in soil. Funct. Ecol. 19, 369–377.
Freedman, Z., Eisenlord, S.D., Zak, D.R., Xue, K., He, Z., Zhou, J., 2013. Towards a molecular understanding of N cycling in northern hardwood forests under future rates of N deposition. Soil Biol. Biochem. 66, 130–138.
Grishkan, I., Jia, R.L., Kidron, G.J., Li, X.R., 2015. Cultivable microfungal communities inhabiting biological soil crusts in the Tengger Desert, China. Pedosphere 25, 351–363.
Huang, W., Liu, J., Wang, Y.P., Zhou, G., Han, T., Li, Y., 2012. Increasing phosphorus limitation along three successional forests in southern China. Plant Soil 364, 181–191.
Jesus, E.D., Marsh, T.L., Tiedje, J.M., Moreira, F.M.D., 2009. Changes in land use alter the structure of bacterial communities in Western Amazon soils. ISME J. 3, 1004–1011.
Kandeler, E., Deiglmayr, K., Tscherko, D., Bru, D., Philippot, L., 2006. Abundance of narG, nirS, nirK, and nosZ genes of denitrifying bacteria during primary successions of a glacier foreland. Appl. Environ. Microbiol. 72, 5957–5962.
Knelman, J.E., Schmidt, S.K., Lynch, R.C., Darcy, J.L., Castle, S.C., Cleveland, C.C., Nemergut, D.R., 2014. Nutrient addition dramatically accelerates microbial community succession. PLoS One 9, e102609.
Li, X.R., Ma, F.Y., Xiao, H.L., Wang, Xin P., Ke, C.K., 2004. Long-term effects of revegetation on soil water content of sand dunes in arid region of Northern China. J. Arid Environ. 57, 1–16.
Li, X.R., Chen, Y.W., Su, Y.G., Tan, H.J., 2006. Effects of biological soil crust on desert insect diversity: evidence from the Tengger Desert of northern China. Arid Soil Res. Rehabil. 20, 263–280.
Li, X.R., He, M.Z., Duan, Z.H., Xiao, H.L., Jia, X.H., 2007a. Recovery of topsoil physicochemical properties in revegetated sites in the sand-burial ecosystems of the Tengger Desert, northern China. Geomorphology 88, 254–265.
Li, X.R., Kong, D.S., Tan, H.J., Wang, X.P., 2007b. Changes in soil and vegetation following stabilisation of dunes in the southeastern fringe of the Tengger Desert, China. Plant Soil 300, 221–231.
Liang, Y.T., Nostrand, J.D.V., Deng, Y., He, Z.L., Wu, L.Y., Zhang, X., Li, G.H., Zhou, J.Z.,

2011. Functional gene diversity of soil microbial communities from five oil-contaminated fields in China. ISME J. 5, 403–413.
Little, A.F., Robinson, C.J., Peterson, S.B., Raffa, K.F., Handelsman, J., 2008. Rules of engagement: interspecies interactions that regulate microbial communities. Annu. Rev. Microbiol. 62, 375–401.
Liu, G., Jiang, N., Zhang, L., Liu, Z., 1996. Soil Physical and Chemical Analysis and Description of Soil Profiles. China Standard Methods Press, Beijing, China (In Chinese).
Liu, Y.M., Li, X.R., Xing, Z.S., Zhao, X., Pan, Y.X., 2013. Responses of soil microbial biomass and community composition to biological soil crusts in the revegetated areas of the Tengger Desert. Appl. Soil Ecol. 65, 52–59.
Liu, L.C., Liu, Y.B., Hui, R., Xie, M., 2017a. Recovery of microbial community structure of biological soil crusts in successional stages of Shapotou desert revegetation, northwest China. Soil Biol. Biochem. 107, 125–128.
Liu, L.C., Liu, Y.B., Zhang, P., Song, G., Hui, R., Wang, J., 2017b. Development of bacterial communities in biological soil crusts along a revegetation chronosequence in the Tengger Desert, northwest China. Biogeosci. Discuss. 14, 3801–3814.
Lozupone, C.A., Knight, R., 2007. Global patterns in bacterial diversity. Proc. Natl. Acad. Sci. 104, 11436–11440.
Nanjing Institute of Soil Sciences, Chinese Academy of Sciences, 1978. Physical and Chemical Analysis Methods of Soils. Shanghai Science Technology Press Shanghai, pp. 7–59 (in Chinese).
Nelson, D.W., Sommers, L.E., 1996. Total carbon, organic carbon, and organic matter. In: Page, A.L. (Ed.), Methods of Soil Analysis Part 3-Chemical Methods, American Society of Agronomy (ASA) Publ. No. 9. ASA, pp. 961–1010.
Nemergut, D.R., Anderson, S.P., Cleveland, C.C., Martin, A.P., Miller, A.E., Seimon, A., Schmidt, S.K., 2007. Microbial community succession in an unvegetated, recently deglaciated soil. Microb. Ecol. 53, 110–122.
Reeve, J.R., Schadt, C.W., Carpenter-Boggs, L., Kang, S., Zhou, J., Reganold, J.P., 2010. Effects of soil type and farm management on soil ecological functional genes and microbial activities. ISME J. 4, 1099–1107.
Richardson, S.J., Peltzer, D.A., Allen, R.B., Mcglone, M.S., Parfitt, R.L., 2004. Rapid development of phosphorus limitation in temperate rainforest along the Franz Josef soil chronosequence. Oecologia 139, 267–276.
Schmidt, S.K., Reed, S.C., Nemergut, D.R., Grandy, A.S., Cleveland, C.C., Weintraub, M.N., Hill, A.W., Costello, E.K., Meyer, A.F., Neff, J.C., 2008. The earliest stages of ecosystem succession in high-elevation (5000 metres above sea level), recently deglaciated soils. Proc. Biol. Sci. 275, 2793–2802.
Tscherko, D., Rustemeier, J., Richter, A., Wanek, W., Kandeler, E., 2003. Functional diversity of the soil microflora in primary succession across two glacier forelands in the Central Alps. Eur. J. Soil Sci. 54, 685–696.
Van Nostrand, J.D., Yin, H.Q., Wu, L.Y., Yuan, T., Zhou, J.Z., 2016. Hybridization of Environmental Microbial Community Nucleic Acids by GeoChip. Springer New York, pp. 183–196.
Vitousek, P.M., 1999. Nutrient limitation to nitrogen fixation in young volcanic sites. Ecosystems 2, 505–510.
Vitousek, P.M., Porder, S., Houlton, B.Z., Chadwick, O.A., 2010. Terrestrial phosphorus limitation: mechanisms, implications, and nitrogen-phosphorus interactions. Ecol. Appl. 20, 505–510.
Wang, J., Bao, J.T., Li, X.R., Liu, Y.B., 2016. Molecular ecology of nifH genes and transcripts along a chronosequence in revegetated areas of the Tengger Desert. Microb. Ecol. 71, 150–163.
Yang, Y.F., Gao, Y., Wang, S.P., Xu, D.P., Yu, H., Wu, L.W., Lin, Q.Y., Hu, Y.G., Li, X.Z., He, Z.L., Deng, Y., Zhou, J.Z., 2014. The microbial gene diversity along an elevation gradient of the Tibetan grassland. ISME J. 8, 430–440.
Yang, S.H., Zhang, Y.G., Cong, J., Wang, M.M., Zhao, M.X., Lu, H., Xie, C.Y., Yang, C.Y., Yuan, T., Li, D.Q., Zhou, J.Z., Gu, B.H., Yang, Y.F., 2017. Variations of soil microbial community structures beneath broadleaved forest trees in temperate and subtropical climate zones. Front. Microb. 8, 1–10.
Yeager, C.M., Kornosky, J.L., Morgan, R.E., Cain, E.C., Garcia-Pichel, F., Housman, D.C., Belnap, J., Kuske, C.R., 2007. Three distinct clades of cultured heterocystous cyanobacteria constitute the dominant N_2-fixing members of biological soil crusts of the Colorado Plateau, USA. FEMS Microb. Ecol. 60, 85–97.
Yue, H.W., Wang, M.M., Wang, S.P., Gilbert, J.A., Sun, X., Wu, L.W., Lin, Q.Y., Hu, Y.G., Li, X.Z., He, Z.L., Zhou, J.Z., Yang, Y.F., 2015. The microbe-mediated mechanisms affecting topsoil carbon stock in Tibetan grasslands. ISME J. 9, 1–9.
Zaady, E., Bouskila, A., 2002. Lizard burrows association with successional stages of biological soil crusts in an arid sandy region. J. Arid Environ. 50, 235–246.
Zhang, B.C., Kong, W.D., Wu, N., Zhang, Y.M., 2016a. Bacterial diversity and community along the succession of biological soil crusts in the Gurbantunggut Desert, northern China. J. Basic Microbiol. 56, 670–679.
Zhang, T., Jia, R.L., Yu, L.Y., 2016b. Diversity and distribution of soil fungal communities associated with biological soil crusts in the southeastern Tengger Desert (China) as revealed by 454 pyrosequencing. Fungal Ecol. 23, 156–163.
Zhou, J.Z., Kang, S., Schadt, C.W., Garten, C.T., 2008. Spatial scaling of functional gene diversity across various microbial taxa. Proc. Natl. Acad. Sci. 105, 7768–7773.
Zhou, J.Z., Xue, K., Xie, J.P., Deng, Y., Wu, L.Y., Cheng, X.L., Fei, S.F., Deng, S.P., He, Z.L., Nostrand, J.D.V., Luo, Y.Q., 2011. Microbial mediation of carbon-cycle feedbacks to climate warming. Nat. Clim. Chang. 2, 106–110 (Nat. Clim. Change 2, 106-110).